DOI: 10.1002/ejoc.200600376

Are Molecular 5,8-π-Extended Quinoxaline Derivatives Good Chromophores for Photoluminescence Applications?

Fabiana S. Mancilha,[a] Brenno A. DaSilveira Neto,[a] Aline S. Lopes,[a] Paulo F. Moreira Jr.,[b] Frank H. Quina,[b] Reinaldo S. Gonçalves,[a] and Jaïrton Dupont*[a]

Keywords: Quinoxalines / Benzothiadiazole / Luminescence / C–C coupling

The synthesis of a new series of photoluminescent compounds, namely 5,8-diaryl quinoxaline derivatives (aryl = phenyl, 4-fluorophenyl, 4-methoxyphenyl, and 4-cyanophenyl), was achieved by a direct Suzuki cross-coupling reaction with the employment of a NCP-pincer palladacycle. The electrochemical and photophysical properties of these compounds were also investigated. Four new 4,8-diaryl-2,1,3-benzothiadiazoles were also synthesized in order to enable a comparison between the two types of nitrogen-containing π-extended heterocycles. The substitution of a hydrogen atom at the 4-position of the aryl that is groups attached to the quinoxaline or benzothiadiazole base by either electron-donating or -withdrawing groups results in an increase in the bandgap energy (from 2.21 to 2.52 eV) of π-extended 5,8-quinoxaline derivatives and a decrease in the bandgap energy (from 2.65 to 2.40 eV) of π-extended 2,1,3-benzothiadiazoles. Moreover, π-extension at the 5- and 8-positions of the quinoxaline core is not essential for the photoluminescence of these compounds and 4,7-π-extended 2,1,3-benzothiadiazole derivatives are far better candidates for luminescence applications than are the quinoxaline derivatives.

(© Wiley-VCH Verlag GmbH & Co. KGaA, 69451 Weinheim, Germany, 2006)

Introduction

Without doubt, π-extended compounds are of great utility in the chemistry of photoluminescent compounds.[1–3] In this respect, the suitable thermal stability, electrochemical (reversible and quasi-reversible electron-transfer processes), and photophysical characteristics (large Stokes shift and high fluorescence quantum yield) are the minimum properties necessary for an organic molecule to be a good candidate for organic light-emitting diode (OLED) applications.[4] Because the electron affinities (EA) and ionization potentials (IP) that define the HOMO–LUMO levels of aromatic molecules are well-correlated with electrochemical reduction and oxidation potentials, the structure-reduction-potential trends – as for example, those presented in Scheme 1 – may provide a first level basis for the selection of new target π-extended-type molecules for synthesis and investigation. Thus, heteroaromatic rings containing only imine nitrogen atoms (C=N) generally have a less negative reduction potential compared with those of analogous aromatic hydrocarbons and heteroaromatic rings that contain oxygen or sulfur atoms. For polycyclic rings, expansion of the π-conjugation system is one method used to increase the reduction potential of the compound. 2,1,3-Benzothiadiazole (IX) and quinoline (VII) are among the most common building blocks used to increase the reduction potential and electron affinity of current electron-transport materials for OLEDs.[5–7]

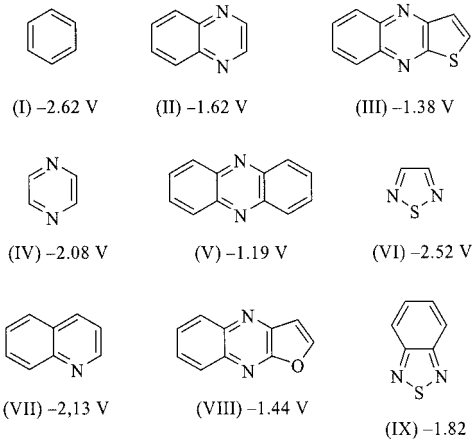

Scheme 1. Structure and half-wave reduction potentials (versus SCE) of some aromatic heterocycles (adapted from ref.[8]).

Quinoxaline (Q) containing building blocks are also extensively used in the chemistry of photoluminescent molecules because they usually display high electron affinities, good thermal stabilities,[9] and they may also act as electron-transporting materials.[10,11] These derivatives have been successfully incorporated into polymers for use as elec-

[a] Laboratory of Molecular Catalysis, Institute of Chemistry, UFRGS,
Av. Bento Gonçalves 9500, Porto Alegre, RS, 91501-970, Brazil
E-mail: dupont@iq.ufrgs.br
[b] Institute of Chemistry – USP,
CP 26.077, São Paulo, SP, 05513-970, Brazil

Supporting information for this article is available on the WWW under http://www.eurjoc.org or from the author.

 © 2006 Wiley-VCH Verlag GmbH & Co. KGaA, Weinheim

tron-transport materials in multilayer OLEDs.[12,13] Several different protocols are available for the synthesis of quinoxalines,[14–17] especially when the extension of the π-conjugation is at the 2- and 3-positions of the quinoxaline unit.[18] Simple π-extension at the 5- and8-positions of the quinoxaline base is difficult to achieve by classical Suzuki and Sonogashira cross-coupling protocols and only one example of a alkynylation reaction between trimethylsilylacetylene and 5,8-diiodoquinoxaline, which proceeded in moderate yield, has been reported so far.[19] Under the same reaction conditions, however, no product was observed when 5,8-dibromoquinoxaline was used as the starting reagent.[19] The synthesis of 5,8-π-extended quinoxaline derivatives is usually carried out through the π-extension of a 2,1,3-benzothidiazole (BTD) derivative, which is then followed by sulfur extrusion and cyclization of the resulting product with the appropriate 1,2-dicarbonyl compound (Scheme 2).[20–22]

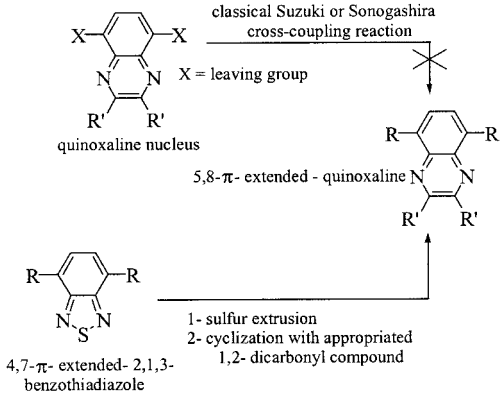

Scheme 2. Possible reaction pathways for the synthesis of 5,8-π-extended quinoxalines with the use of 4,7-π-extended benzothiadiazoles.

Herein we describe the synthesis, characterization, and the photophysical and electrochemical properties of a new series of 5,8-π-extended quinoxaline derivatives and 4,7-π-extended 2,1,3-benzothiadiazole-derivatives which can be obtained by Suzuki coupling with the employment of a specific NCP-pincer-type palladacycle as a catalyst precursor. The efficiency of the photoluminescence of these compounds and their electrochemical behavior is compared to that of a new series of 4,7-π-extended 2,1,3-benzothiadiazoles and 5,8-π-extended quinoxaline derivatives.

Results and Discussion

Our strategy for the synthesis of the desired Q and BTD compounds involved the treatment of commercially available *o*-phenylenediamine (**1**) with freshly distilled thionyl chloride in the presence of triethylamine in CH_2Cl_2 as the solvent to afford 2,1,3-benzothiadiazole (**2**) in 93% yield after steam distillation.[23–25] The reaction of **2** with molecular bromine (added dropwise very slowly) in hydrobromic acid exclusively affords 4,7-disubstituted regioisomer **3** in 95% yield (Scheme 3).[26]

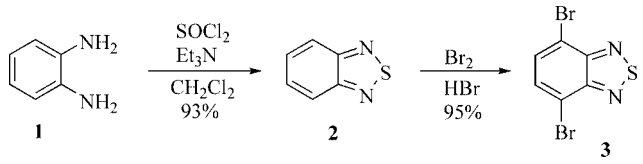

Scheme 3. Synthesis of 4,7-dibromo-2,1,3-benzothiadiazole (**3**).

The sulfur extrusion reaction of compound **3** can be performed by three different methodologies depending on the scale of the reaction (Scheme 4). The resultant *o*-aromatic diamine is then immediately treated with glyoxal sodium bisulfite to afford air-stable quinoxaline **5** (Scheme 4) in 76% yield after purification.

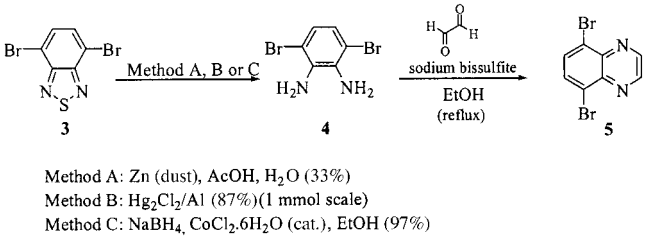

Scheme 4. Reductive sulfur extrusion reaction of 2,1,3-benzothiadiazole **3** and formation of 5,8-dibromoquinoxaline **5**.

In order to prepare diamine **4**, which was necessary for the synthesis of desired quinoxaline intermediate **5**, we initially attempted some published protocols for the reductive extrusion of sulfur [27,28] from **3**,[29–31] but **4** was only obtained in moderate yields or the reaction was limited to a 1 mmol scale. However, the reductive extrusion of sulfur from **3** could be easily achieved with the reductive system of $NaBH_4/CoCl_2{\cdot}6H_2O$ (cat.)/EtOH to produce desired diamine **4** in 97% yield.[31]

The classical Suzuki cross-coupling protocol[32] between **5** and arylboronic acids, which employs $Pd(PPh_3)_4$ and Na_2CO_3, results in almost no product. However, the use of a specific, recently developed NCP-pincer palladacycle[33,34] results in new photoluminescent 5,8-π-extended disubstituted quinoxaline derivatives **6** in excellent yields (Scheme 5).

As an alternative route, we first synthesized photoluminescent π-extended BTDs **7a**–**d** that can also be of great interest for the chemistry of OLEDs as we have described for other BTD series.[35] Thereafter, sulfur extrusion of **7** followed by cyclization resulted in 5,8-π-extended quinoxaline derivatives **6a**–**d**.

A direct Suzuki coupling reaction of **5** and the NCP-pincer palladacycle proved to be a superior synthetic strategy to that of the sulfur extrusion–cyclization sequence. Although the sulfur extrusion reactions gave high yields (Scheme 5), the cyclization reactions afforded compounds **6a**–**d** in only moderate yields (Scheme 5). In the case of compound **7d**, the CN group was partially reduced to the corresponding primary amine during the sulfur extrusion reaction. The yields of the compounds synthesized by direct Suzuki coupling and those obtained by the sulfur extrusion process followed by cyclization are summarized in Table 1.

 © 2006 Wiley-VCH Verlag GmbH & Co. KGaA, Weinheim

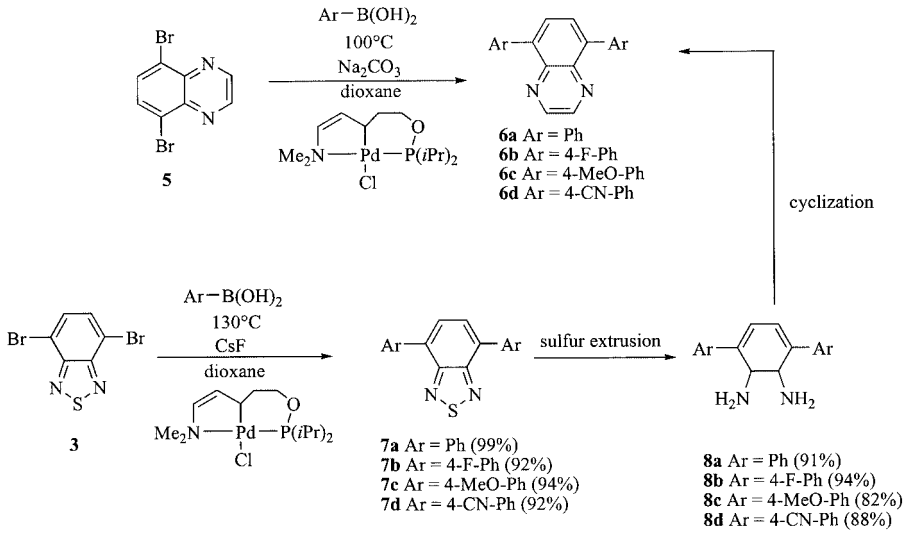

Scheme 5. Synthesis of photoluminescent π-extended compounds **6a**–**d** and **7a**–**d**.

Table 1. Yields for compounds **6a**–**d** synthesized by direct Suzuki coupling and the aforementioned indirect route.

Compound	Yield [%]	
	Direct Suzuki	Indirect route[a]
6a	95	65
6b	87	63
6c	99	61
6d	91	57

[a] Yield is over two steps – sulfur extrusion and cyclization reactions.

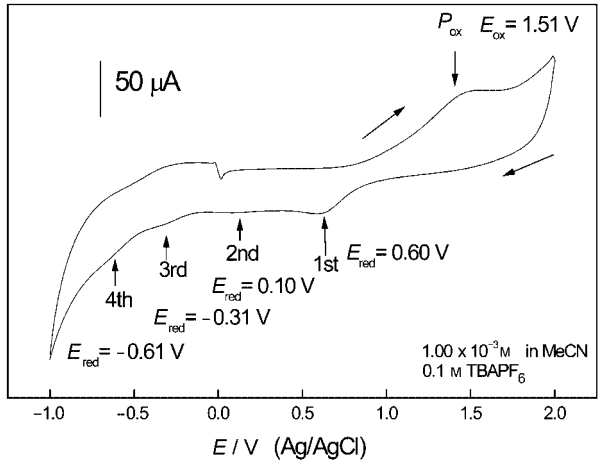

Figure 1. Cyclic voltammogram of compound **6a** (1 mM solution) in MeCN recorded at a scan rate of 200 mV/s.

The cyclic voltammograms (CV) of the compounds investigated were recorded with the procedures used previously for this type of compound. Current versus potential curves were employed to characterize the charge transfer process that occurs at the electrode surface that is due to the oxidation–reduction of the compounds. The strategy adopted was to start the voltammograms at 0.0 V in order to avoid any charge transfer processes at the beginning of the experiment.

Figure 1 shows the CV of compound **6a** at the platinum electrode recorded at a potential sweep rate of 200 mV/s. Compound **6a** possesses a large electrochemical window: from –1.0 V to 2.0 V (Ag/AgCl) for the anodic and cathodic potential sweeps, respectively. During the anodic potential sweep, there is a well-defined peak (1.51 V) associated with the electrooxidation of the compound. In contrast, during the cathodic potential sweep, four potential peaks are present.

The first (0.60 V)of these four peaks is related to the electrochemical oxidation peak (1.51 V) and indicates a quasi-reversible process. The other three potential peaks (0.10 V, –0.31 V, and –0.61 V) are attributed to irreversible electroreduction processes that involve species that are irreversibly formed on the electrode surface. Compound **6a** is therefore a potential candidate for inclusion in an electron-transporting layer of an organic light-emitting device because the quasi-reversible oxidation process should allow it to undergo one-electron oxidization and reduction without decomposition.[36]

The same experiment repeated with compound **7a** revealed a completely different electrochemical behavior, as shown in Figure 2.

In this case, the charge transfer processes occur over a somewhat narrower potential range from –1.9 V to –0.80 V. The oxidation–reduction potential peaks observed at –1.27 V during the anodic potential sweep and at –1.43 V (Ag/AgCl) during the cathodic potential sweep are indicative of a quasi-reversible process, which apparently involves a single-electron transfer. A plausible mechanism for the electrochemical behavior of 2,1,3-BTD derivatives has been presented by Hirao et al.[21] Because adsorption of the compounds on the electrode surface plays an important role in the charge transfer processes, the difference between **6a** and **7a** may reflect the greater propensity of sulfur-containing BTD derivative **7a** to adsorb at the electrode surface compared with that of quinoxaline derivative **6a**.

 © 2006 Wiley-VCH Verlag GmbH & Co. KGaA, Weinheim

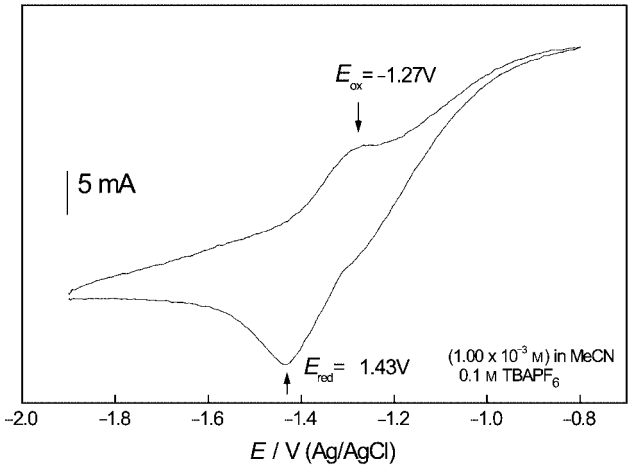

Figure 2. Cyclic voltammogram of compound **7a** (1 mM solution) in MeCN recorded at a scan rate of 200 mV/s.

The introduction of two electron-withdrawing fluorine atoms in structure **6b** results in only a small modification of the electrochemical behavior of **6b** relative to that of **6a**, as shown in Figure 3.

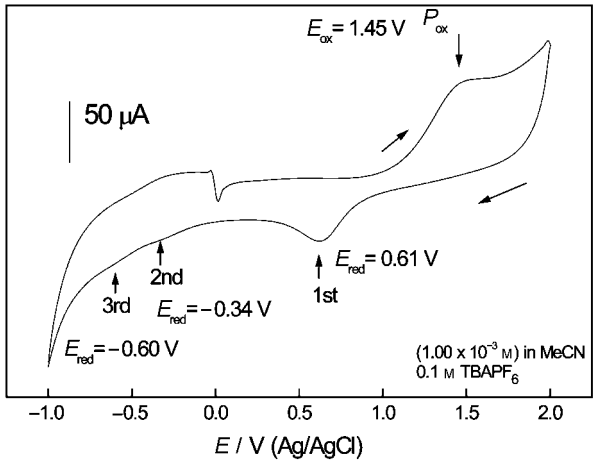

Figure 3. Cyclic voltammogram of compound **6b** (1 mM solution) in MeCN recorded at a scan rate of 200 mV/s.

During the anodic potential sweep, one oxidation process was observed at 1.45 V. The first peak observed during the cathodic potential sweep (0.61 V) is the corresponding reduction process of the oxidized species formed on the electrode surface. The other potential peaks (–0.34 V and –0.60 V) are attributed to multielectron irreversible reduction of the adsorbed species. Once again, quasi-reversible behavior is observed only in the oxidation process, which restricts the use of **6b** to the electron-transporting layer of an organic light emitting device.

The cyclic voltammogram of compound **7b** exhibits two close-lying potential peaks during the anodic potential sweep and two potential peaks during the cathodic potential sweep, as shown in Figure 4.

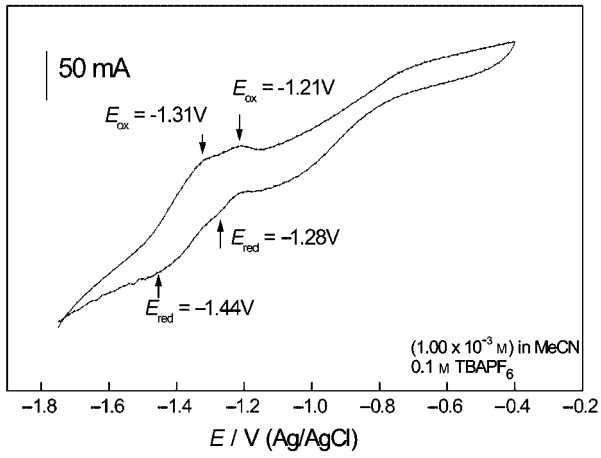

Figure 4. Cyclic voltammogram of compound **7b** (1 mM solution) in MeCN recorded at a scan rate of 200 mV/s.

The charge transfer processes occurring at –1.21 V and –1.28 V are reversible, while those at –1.44 V and –1.31 V correspond to a quasi-reversible process. From the comparison of **7a** with **7b**, it is clear that the introduction of the F atoms alters the charge transfer process and favors a multielectron step. Relative to **6b**, the electrochemical behavior of 2,1,3-benzothiadiazole **7b** is much more amenable to the potential application as an OLED device.

The incorporation of two electron-donating groups (MeO) into the structure of **6c** leads to remarkable modifications in the oxidation–reduction processes, as shown in the current versus potential curves presented in Figure 5.

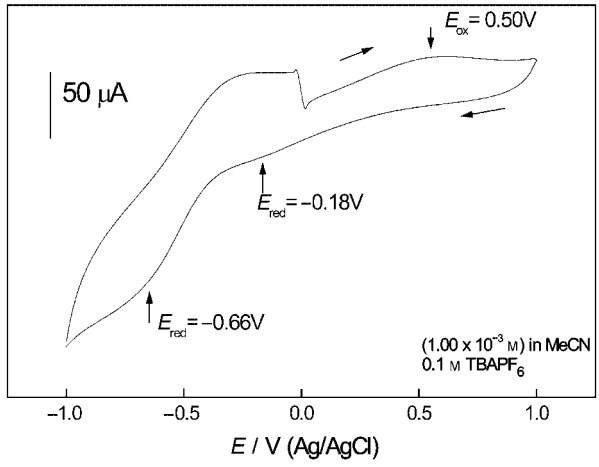

Figure 5. Cyclic voltammogram of compound **6c** (1 mM solution) in MeCN recorded at a scan rate of 200 mV/s.

The charge transfer processes of **6c** occur over a much narrower range than they do for either **6a** or **6b**. The MeO groups may affect the energy required for charge transfer, or the affinity, of this compound for adsorption onto the electrode surface. The oxidation–reduction potential peaks (0.50 V and –0.18 V) are associated with a quasi-reversible charge transfer process, whereas the last potential peak involves an irreversible process. As expected, the presence of electron-donating groups has a direct influence on the re-

 © 2006 Wiley-VCH Verlag GmbH & Co. KGaA, Weinheim

duction of the compound, which results in a net cathodic shift of the cyclic voltammogram of compound **6c**.

In structure **7c**, the same electron-donating methoxy groups induce a large modification in the voltammogram, as shown in Figure 6.

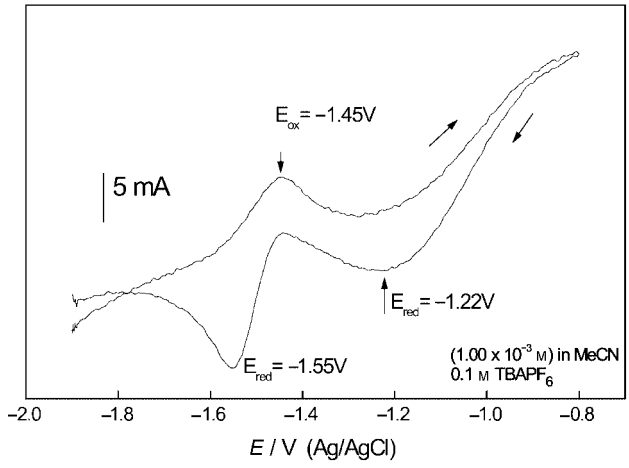

Figure 6. Cyclic voltammogram of compound **7c** (1 mM solution) in MeCN recorded at a scan rate of 200 mV/s.

The oxidation–reduction potential peaks (–1.45 V and –1.55 V) are associated with quasi-reversible charge transfer processes. The MeO groups induce a shift of both processes to more negative potential values relative to those of **7a** and **7b**. However, multielectron reduction steps are involved during the cathodic potential sweep. In **6c**, these processes were shifted to more positive potentials and the last charge transfer irreversibly produced new species on the electrode surface. In **7c**, the electron transfer is observed at more negative potentials and is a reversible process.

The presence of two electron-withdrawing groups (CN) in compound **6d** does not cause significant modifications of the voltammogram relative to **6a**–**c**, as observed in Figure 7.

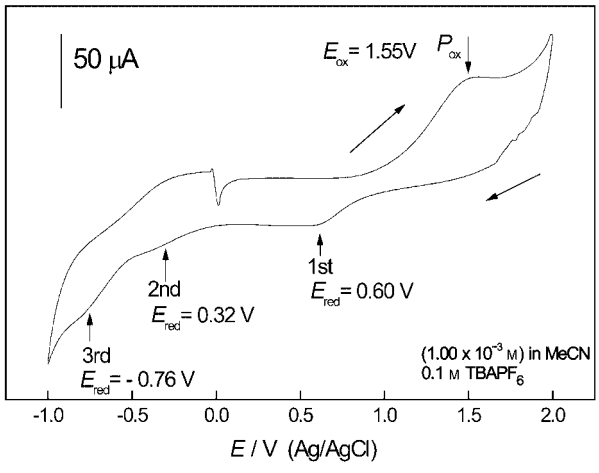

Figure 7. Cyclic voltammogram of compound **6d** (1 mM solution) in MeCN recorded at a scan rate of 200 mV/s.

This behavior is similar to that observed in structures **6a** and **6b** and the same comments should be applied here. A quasi-reversible process is observed in the oxidative sweep (potential peak at 1.55 V, related to the reduction peak at 0.60 V). The other two cathodic processes (0.32 V and –0.76 V) are irreversible.

This is in contrast to **7d**, where the presence of the CN groups induces a significant modification in the cyclic voltammogram, as shown in Figure 8.

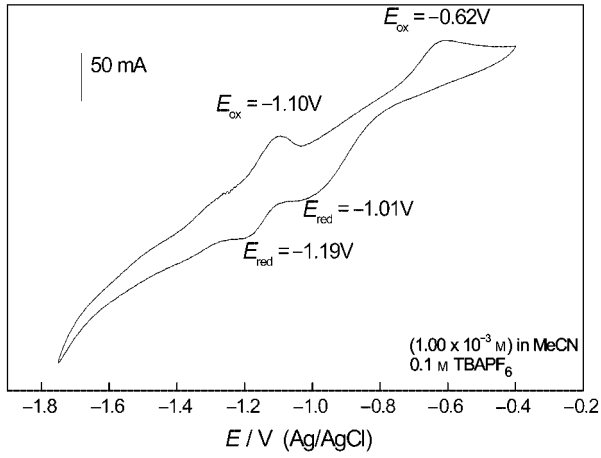

Figure 8. Cyclic voltammogram of compound **7d** (1 mM solution) in MeCN recorded at a scan rate of 200 mV/s.

The electrochemical charge transfer processes were remarkably changed by the presence of a CN group on the structures when we compare compound **7d** with **7a**–**c**. A well-defined reversible oxidation–reduction process was observed at the potential peaks –1.10 V and –1.19 V, and a quasi-reversible process was observed at the potential peaks –0.62 V and –1.01 V. This effect is comparable to those observed with compound **7b**. The comparison between compounds **6d** and **7d** reinforces the significant differences in the electrochemical behavior of the BTD and Q derivatives. A systematic study of the substituent effects on the electrochemical properties combined with an approach to assess structure–property relationships was previous reported.[37]

All four BTDs have a small electrochemical window and almost all processes are reversible or quasi-reversible in both the oxidation and the reduction pathways. The results suggest the possibility that these compounds can be used for both hole- and electron-transport, as required in a single-layer electroluminescent device.[35] The four Q derivatives, however, exhibit irreversible multielectron reduction processes and a quasi-reversible oxidation process. This restricts the possibility of their use to that of an electron-transporting layer in an OLED but not as a hole-transporting layer.[36]

The photophysical properties of all of the compounds were also investigated and the results are summarized in Table 2.

All BTD compounds have rather good fluorescence quantum yields, especially **7a** (Φ_f = 0.80) and **7b** (Φ_f = 0.71), and show Stokes shifts between 67–108 nm. The lowest energy absorption bands (in acetonitrile) are assigned to π–π* transitions by virtue of their large molar extinction coefficients (log ε values in the range of 3.52–4.12). In con-

 © 2006 Wiley-VCH Verlag GmbH & Co. KGaA, Weinheim

Table 2. UV/Vis and fluorescence data for compounds **6a**–**d** and **7a**–**d**.

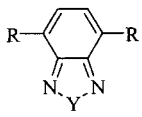

Y = HC=CH
Q (quinoxaline)
R = Ph, **6a**
R = 4-F-Ph, **6b**
R = 4-MeO-Ph, **6c**
R = 4-CN-Ph, **6d**

Y = S
BTD (2,1,3 benzothiadiazole)
R = Ph, **7a**
R = 4-F-Ph, **7b**
R = 4-MeO-Ph, **7c**
R = 4-CN-Ph, **7d**

	Cpd. type	log ε[a]	λ_{abs}^{max} [nm][a]	λ_{abs}^{max} [nm][b]	λ_{em}^{max} [nm][b]	Stokes shift [nm][b]	E_{gap}^{op} [eV][c]	Φ_f [d]	τ_f (sing) [ns][e]	τ_T (trip) [μs][f]	k_q (trip) [$M^{-1}s^{-1}$][g]
6a	Q	3.91	311	467	557	90	2.21	0.051	18.1	27	1.2×10^9
6b		4.84	312	428	489	61	2.43	0.048	17.4	27	ND[h]
6c		3.11	312	427	473	46	2.52	0.099	12.9	2.3	1.4×10^9
6d		4.55	311	419	476	57	2.32	0.094	12.3	2.9	0.8×10^9
7a	BTD	4.04	402	426	493	67	2.65	0.80	12.2	–[i]	–[h]
7b		3.62	372	443	495	52	2.54	0.71	14.6	–[i]	–[h]
7c		3.52	362	418	526	108	2.40	0.51	12.7	–[i]	–[h]
7d		4.12	356	419	503	84	2.53	0.58	6.2	–[i]	–[h]

[a] MeCN solution (1.0000×10^{-5} M). [b] Solid-state. [c] Energy of the bandgap (optical – from solid-state). [d] Quantum yield of fluorescence [quinine sulfate (from Riedel-de Haën) in 1 M H_2SO_4, Φ_f = 0.55, as standard]. [e] Singlet lifetime, determined by single photon counting. [f] Triplet lifetime, determined by nanosecond laser flash photolysis in acetonitrile in the absence of oxygen. [g] Bimolecular rate constant for oxygen quenching of the triplet state, determined as $[1/\tau_T(air) - 1/\tau_T(nitrogen)] = k_q [O_2]$, where $[O_2] = 1.9\times10^{-3}$ M in air-saturated acetonitrile.[37] [h] Not determined, signal too weak to determine lifetime adequately in the presence of oxygen. [i] Not determined, transient signals weak and indicative of complex, wavelength-dependent kinetics.

trast, all Q derivatives have low fluorescence quantum yields but show large Stokes shifts (57–90 nm). The lowest energy absorption bands (in acetonitrile) are assigned to π–π* transitions by virtue of their molar extinction coefficients (logε values in the range of 3.11–4.84). In solution, the λ_{abs}^{max} is very close for all four Q compounds, but very distinct in all BTD systems. The absorption (λ_{abs}^{max}) and emission (λ_{em}^{max}) maxima (in solid state) lie between 419–468 nm and 473–557 nm, respectively. Compounds **6a**, **7c**, and **7d** have large Stokes shifts: 90, 108, and 84 nm, respectively. This indicates a very efficient intramolecular charge transfer (ICT) in the excited state between the terminal CN group (electron-withdrawing), or the MeO group (electron-donating), and the core employed, which in this case is a BTD-type compound. In the Q-type compounds, the addition of electron-donating or -withdrawing groups has a similar effect on the ICT, and the compounds possibly present a very efficient process. These characteristics are required in the solid-state of the potential candidates so that an OLED test can be run.

Compounds **6a**–**d** show relatively strong triplet–triplet absorption by laser flash photolysis (355 nm excitation, Nd-YAG laser) in the absence of oxygen, with triplet lifetimes in the range of 2.3–27 μs, which suggests that there is efficient intersystem crossing in these four compounds. The lack of noticeable laser-induced decomposition also indicates high chemical stability in the excited state in the absence of oxygen. The triplet states of **6a**–**d** are efficiently quenched by molecular oxygen (presumably by energy transfer to form singlet oxygen). In acetonitrile, the bimolecular rate constants for the quenching of **6** by oxygen ($0.8–1.4\cdot10^9$ $M^{-1}s^{-1}$, Table 2) are similar to those reported for naphthalene derivatives with electron-withdrawing substituents.[38] Compounds **7a**–**d** exhibited weak transient signals with complex, wavelength-dependent kinetics, which were not further investigated.

The bandgap energies were determined from the solid-state absorption spectra. The HOMO–LUMO levels of π-extended conjugated molecules are defined by their electron affinities (EA) and ionization potentials (IP), which are correlated with electrochemical reduction and oxidation potentials or with the energy of the onset of absorption spectra in the solid state.[8] The bandgap energies are all between 2.21 eV and 2.65 eV, a range that is appropriate for application in OLED devices.[39–42]

Figure 9 shows the normalized absorption and emission spectra of the quinoxaline derivative **6a** and the benzothiadiazole derivative **7a** in the solid-state.

Under these conditions, the absorption maximum of **6a** is bathochromically shifted relative to that of **7a** (467 nm for **6a** versus 427 nm for **7a**). In solution, however, the opposite behavior is observed, with a λ_{abs}^{max} of 311 nm and 402 nm for **6a** and **7a**, respectively. The Stokes shift in the solid state is much larger for **6a** (90 nm) than it is for **7a** (65 nm), but the relative fluorescence yield of **7a** is much higher than that of **6a** (see Supporting Information). The energy of the bandgap (HOMO–LUMO) is similar for the two compounds (2.21 eV and 2.65 eV, respectively). The small bandgap energies of these compounds are a very desirable characteristic for a component of OLEDs for customization of the energy use.

Figure 10 presents the normalized absorption and emission spectra of **6b** and **7b** in the solid state.

The fluorine atoms induce a bathochromic shift in the spectra of both **6b** and **7b** (λ_{abs}^{max} of 428 nm and 443 nm, respectively). Both possess large Stokes shifts (61 nm and 52 nm, respectively) and reasonable ICT processes. As before, the relative fluorescence yield of **7b** is much higher

 © 2006 Wiley-VCH Verlag GmbH & Co. KGaA, Weinheim

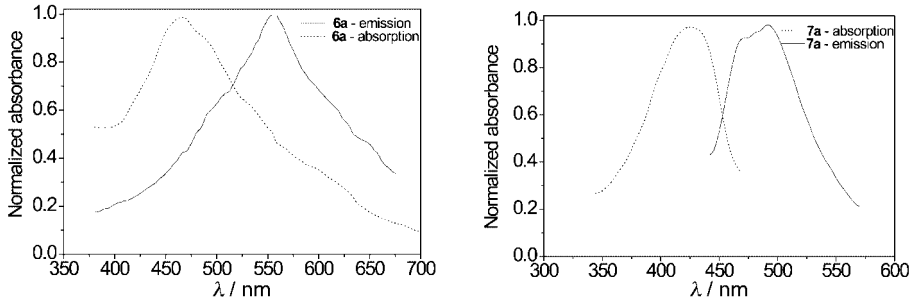

Figure 9. Absorption (dashed curve) and fluorescence emission (solid curve) spectra of **6a** (left) and **7a** (right) in the solid-state.

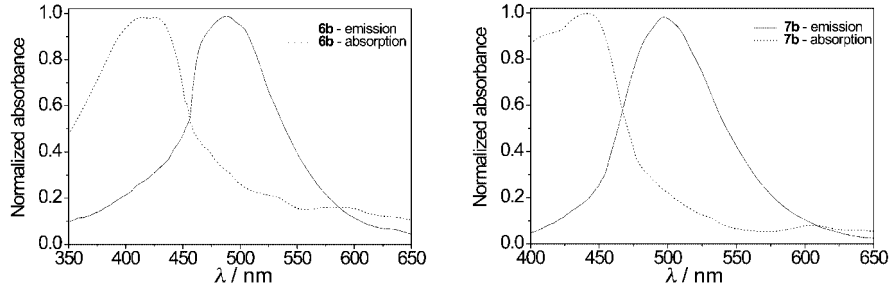

Figure 10. Absorption (dashed curve) and fluorescence emission (solid curve) spectra of **6b** (left) and **7b** (right) in the solid state.

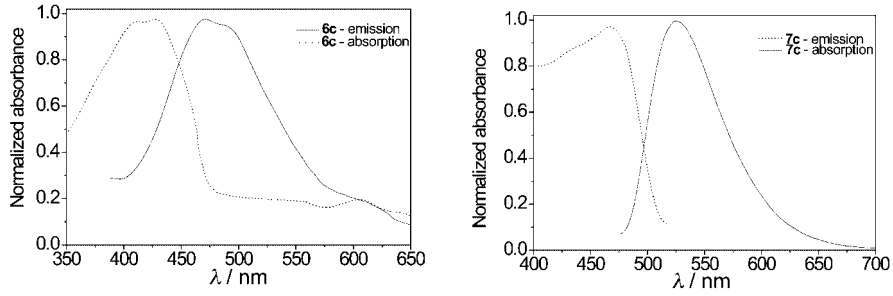

Figure 11. Absorption (dashed curve) and fluorescence emission (solid curve) spectra of **6c** (left) and **7c** (right) in the solid state.

than that of **6b** (see Supporting Information). The energy of the bandgap is similar in both compounds (2.43 eV and 2.54 eV, respectively). In comparison with **6a** (2.21 eV), the insertion of two fluorine atoms increases the bandgap energy of **6b** (2.43 eV), but, relative to **7a** (2.65 eV), the fluorides diminish the energy of the bandgap in **7b** (2.54 eV).

Figure 11 shows the normalized absorption and emission spectra of **6c** and **7c** in the solid state.

A similar redshift is noted when a MeO group is attached to the compound, as in compounds **6c** and **7c**. The λ_{abs}^{max} of **6c** and **7c** is 427 nm and 418 nm, respectively. Both possess large Stokes shifts (46 nm and 108 nm, respectively). The large Stokes shift for compound **7c** implies that this compound exhibits very efficient ICT. Once again, the fluorescence intensity of the BTD core is much higher than that of the Q core (see Supporting Information). The energy of the bandgap is similar in both compounds (2.52 eV and 2.40 eV, respectively). However, in the case of Q **6a** (2.21 eV), the inclusion of an electron-donating group increases the bandgap energy (2.52 eV for Q **6c**). In comparison, the energy of the bandgap of BTD **7a** (2.65 eV) diminishes in the presence of the same electron-donating group (2.40 eV for **7c**).

These facts indicate that even in the presence of an electron-donating or -withdrawing group, the substitution of a hydrogen atom for another group results in an increase in the bandgap energy of 5,8-π-quinoxaline-extended compounds and lowers the bandgap energy of π-extended 2,1,3-benzothiadiazole derivatives (Table 2).

Figure 12 shows the solid-state (normalized) absorption and emission spectra of quinoxaline derivative **6d** and benzothiadiazole derivative **7d**. The inclusion of another electron-withdrawing group (CN) leads to equal λ_{abs}^{max} in the solid-state for both compounds. The λ_{abs}^{max} is 419 nm for both compounds. Both possess large Stokes shifts (57 nm and 84 nm, respectively) and a good ICT process. In solution, we observe a redshift in the spectra of compounds **6d** and **7d**. The λ_{abs}^{max} is now 311 nm for quinoxaline containing **6d** and 356 nm for benzothiadiazole containing **7d**. The fluorescence intensity of the BTD core is much higher than that of the Q core (see Supporting Information). The energy of the bandgap is close in both compounds (2.32 eV and

 © 2006 Wiley-VCH Verlag GmbH & Co. KGaA, Weinheim

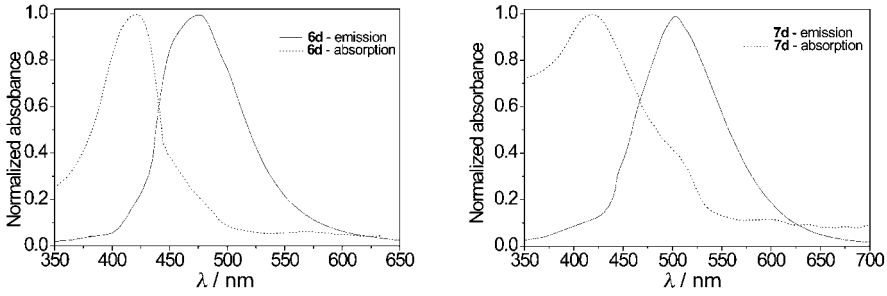

Figure 12. Absorption (dashed curve) and fluorescence emission (solid curve) spectra of **6d** (left) and **7d** (right) in the solid state.

2.53 eV, respectively). In the case of Q **6a** (2.21 eV) the insertion of a CN group once more increases the bandgap energy (2.32 eV for **6d**). When compared to BTD **7a** (2.65 eV) the presence of a CN group lowers the energy of the bandgap (2.53 eV for **7d**).

These observations of **6a**–**d** and **7a**–**d** (Table 2) imply that the substitution of the hydrogen atom at the 4-position of an aryl group by either electron-donating or -withdrawing groups results in an increase in the bandgap energy of 5,8-π-extended quinoxaline derivatives but a decrease in that of π-extended 2,1,3-benzothiadiazoles.

Conclusions

The synthesis of a new series of photoluminescent compounds, namely 5,8-diaryl quinoxaline and 4,7-diaryl-2,1,3-benzothiadiazole derivatives (aryl = phenyl, 4-fluorophenyl, 4-methoxyphenyl, and 4-cyanophenyl) was achieved by a direct Suzuki cross-coupling reaction with the employment of a NCP-pincer palladacycle. The obtained photophysical and electrochemical properties indicate that the substitution of the hydrogen atom at the 4-position of the aryl group that is attached to the quinoxaline or benzothiadiazole core by either electron-donating or -withdrawing groups results in an increase in the bandgap energy of 5,8-π-extended quinoxaline derivatives but a decrease in that of π-extended 2,1,3-benzothiadiazoles. Moreover, the π-extension at the 5- and 8-positions of the quinoxaline base is not essential for the photoluminescence of these compounds. 4,7-π-Extended 2,1,3-benzothiadiazole derivatives were found to be far better candidates for luminescence applications than were the quinoxaline derivatives.

Experimental Section

General: All catalytic reactions were carried out under an argon or nitrogen atmosphere in oven-dried resealable Schlenk tubes. All substrates were purchased from Acros or Aldrich and used without further purification. The NCP palladacycle catalyst precursor was prepared according to the reported method.[33] All new compounds were fully characterized after purification. NMR spectra were recorded with Varian Inova 300 MHz or Varian Gemini 200 MHz spectrometers. Infrared spectra were registered with a Bomem B-102 spectrometer. Melting points were measured with a 12000 PL-DSC apparatus at a heating rate of 5 °C/min or with an Electrothermal IA9000 Melting Point apparatus. Cyclic voltammograms (CV) were recorded with an Autolab PGSTAT 30 Potentiostat. UV/Vis absorption spectra were measured with a Cary 50 Varian spectrophotometer or a Shimadzu Model UV-1601PC. For fluorescence quantum yields, a Shimadzu UV-1601PC spectrophotometer and a Hitachi Model F-4500 spectrofluorometer were employed. Fluorescence decays were collected by the time-correlated single photon counting technique with an Edinburgh Analytical Instruments FL900 lifetime Spectrometer (H_2 lamp excitation source). Lifetimes were determined from the decays with the FL900 convolution and fitting routines for mono- and bi-exponential decay. Nanosecond laser flash photolysis experiments were performed at 20 °C on air-equilibrated solutions and on solutions deoxygenated by exhaustive purging with solvent-vapor-saturated argon in cuvettes capped with a rubber septum. The Edinburgh Analytical Instruments LP900 laser flash photolysis system was equipped with a 450-W Xe high-pressure monitoring lamp and excitation was carried out with the third harmonic (355 nm) of a Surelite II-10 Nd-YAG laser. Solutions were stirred between each laser shot and 10 laser shots were averaged to obtain the transient absorption decays. Solutions were monitored for laser-induced decomposition by conventional UV/Vis absorption spectroscopy (Hewlett–Packard 8452A diode array spectrometer) and replaced by fresh solutions at the first sign of decomposition. The standard exponential decay routines of the LP900 system software were used to analyze the decays of the transient species and to obtain the lifetimes of the excited species. Elemental analyses were performed by the Analytical Center of the Institute of Chemistry – UNICAMP (Brazil).

General Procedure for the Synthesis of 2,1,3-Benzothiadiazole (2): To a 1000 mL flask were added commercial *o*-phenylenediamine (**1**, 10.0 g, 92.5 mmol), CH_2Cl_2 (300 mL), and triethylamine (37.4 g, 370 mmol). The solution was stirred until total dissolution of diamine **1** was observed. Thionyl chloride (184.9 mmol, 2 equiv.) was added dropwise very slowly, and the mixture was heated at reflux for 5 h. The solvent was removed under reduced pressure, and water (700 mL) was added. Concentrated HCl was added to achieve a final pH of 1. Water was added to the reaction mixture, and the desired compound was purified by direct steam distillation. The steam distilled mixture was extracted with CH_2Cl_2 (5 × 200 mL), dried with $MgSO_4$, and filtered. The solvent was removed to afford pure **2** in 93% yield (11.7 g, 86 mmol). ^{1}H NMR (200 MHz, $CDCl_3$): δ = 7.99 (dd, J = 3.2 Hz and J = 5.7 Hz, 2 H), 7.57 (dd, J = 3.2 Hz and J = 5.7 Hz, 2 H) ppm. ^{13}C NMR (50 MHz, $CDCl_3$): δ = 154.6, 129.1, 122.4 ppm. FTIR (KBr): $\tilde{\nu}$ = 1659, 1433, 1264, 1104, 747 cm^{-1}. M.p. 43.6–44.4 °C (ref.[23] 44 °C). $C_6H_4N_2S$ (136.2): calcd. C 52.92, H 2.96, N 20.57, S 23.54; found C 52.63, H 2.74, N 20.31.

General Procedure for the Synthesis of 4,7-Dibromobenzothiadiazole (3): To a 500 mL two-necked round-bottomed flask were added benzothiadiazole **2** (10.0 g, 73.4 mmol) and HBr (150 mL, 48%). A solution containing Br_2 (35.2 g, 220.3 mmol) in HBr (100 mL) was

 © 2006 Wiley-VCH Verlag GmbH & Co. KGaA, Weinheim

added dropwise very slowly (*slow addition is essential!*). If necessary, an additional 100 mL of HBr can be added to the solution. After the total addition of Br_2, the solution was heated at reflux for 6 h. Precipitation of a dark orange solid was noted. The mixture was cooled to room temp., and a sufficient amount of a saturated solution of $NaHSO_3$ was added to completely consume any excess Br_2. The mixture was filtered under vacuum and washed exhaustively with water. The solid was then washed once with cold Et_2O and dried under vacuum for ca. 20 h to afford dibrominated product **3** in 95% yield (20.5 g, 69.8 mmol). ^{1}H NMR (200 MHz, $CDCl_3$/[D_6]DMSO, 8:2): δ = 7.73 (s, 2 H) ppm. ^{13}C NMR (50 MHz, $CDCl_3$/[D_6]DMSO, 8:2): δ = 152.6, 132.1, 113.6 ppm. M.p. 189–190 °C (ref.[26] 188–189 °C). $C_6H_2Br_2N_2S$ (294.0): calcd. C 24.52, H 0.69, Br 54.36, N 9.53, S 10.91; found C 24.78, H 0.76, N 9.72.

Compound **4** was synthesized according to a previously described procedure. The sulfur extrusion reactions of BTDs **7a**–**d**, followed by cyclization, were performed according to a literature method.

General Procedure for the Synthesis of 5,8-Dibromoquinoxaline (5) and Cyclization Reactions: Compound **4** (365 mg, 1.4 mmol) was dissolved in EtOH (10 mL). While the solution was stirred, glyoxal sodium bisulfite (912 mg, 3.4 mmol) was added, and the mixture was heated at reflux for 3 h. The solvent was then removed, and the crude product was washed with water (3 × 20 mL). The yellow solid was then crystallized from hot EtOH to afford compound **5** in 76% yield. ^{1}H NMR (300 MHz, [D_6]DMSO): δ = 9.13 (s, 2 H), 8.17 (s, 2 H) ppm. ^{13}C NMR (75 MHz, [D_6]DMSO): δ = 147.3, 140.6, 133.9, 123.4 ppm. M.p. 229 °C (ref.[43] 226–228 °C). HRMS: calcd. for $C_8H_4Br_2N_2$ 285.87412; found 285.8750.

General Procedure for the Suzuki Coupling Reactions: An oven-dried resealable Schlenk tube was evacuated and back-filled with Ar and charged with CsF (3.7 mmol – for BTD) or Na_2CO_3 (3.7 mmol – for Q), arylboronic acid (3.7 mmol), and the NCP-pincer palladacycle (1–3 mol-%). Compound **3** (1.7 mmol – BTD) or **5** (1.7 mmol – Q) was added in 1,4-dioxane (5 mL). The reaction mixture was stirred and heated at 130 °C (for BTD) or 100 °C (for Q) for 18 h. The solution was then cooled to room temp., and the solvent was evaporated under reduced pressure. The crude material was chromatographed directly on silica gel with Et_2O as the eluent.

Quinoxaline 6a: ^{1}H NMR (300 MHz, $CDCl_3$): δ = 7.96 (d, J = 8.40 and J = 1.18 Hz, 4 H), 7.81 (s, 2 H), 7.56 (m, 4 H), 7.45 (t, J = 7.52 Hz, 2 H) ppm. ^{13}C NMR (75 MHz, $CDCl_3$): δ = 146.0, 141.5, 135.6, 132.6, 127.9 ppm. FTIR (KBr): $\tilde{\nu}$ = 2243, 2122, 802, 795 cm^{-1}. M.p. 181 °C. HRMS: calcd. for $C_{20}H_{14}N_2$ 282.1157; found 282.1131. $C_{20}H_{14}N_2$ (282.3): calcd. C 85.08, H 5.00, N 9.92; found C 84.90, H 4.75, N 10.13.

Quinoxaline 6b: ^{1}H NMR (200 MHz, $CDCl_3$): δ = 7.90–7.62 (m, 4 H), 7.06–7.02 (m, 4 H) ppm. ^{13}C NMR (50 MHz, [D_6]DMSO): δ = 165.3, 162.2, 147.3, 136.6, 136.5, 134.0, 114.5, 114.2 ppm. FTIR (KBr): $\tilde{\nu}$ = 2893, 2659, 2245, 2122, 2054, 1591, 1546, 1487, 801 cm^{-1}. M.p. 147 °C. HRMS: calcd. for $C_{20}H_{12}F_2N_2$ 318.0968; found 318.0991. $C_{20}H_{12}F_2N_2$ (318.3): calcd. C 75.46, H 3.80, N 8.80; found C 75.51, H 3.49, N 8.65.

Quinoxaline 6c: ^{1}H NMR (300 MHz, $CDCl_3$): δ = 9.00 (s, 2 H), 8.15 (d, J = 8.4 Hz, 4 H), 7.99 (s, 2 H), 7.01 (d, J = 8.4 Hz, 4 H), 3.89 (s, 6 H) ppm. ^{13}C NMR (75 MHz, $CDCl_3$): δ = 163.1, 162.0, 146.0, 141.6, 137.5, 133.7, 113.5, 55.2 ppm. FTIR (KBr): $\tilde{\nu}$ = 2644, 2117, 2038, 1591, 1488, 799 cm^{-1}. M.p. 152 °C. HRMS: calcd. for $C_{22}H_{18}N_2O_2$ 342.1368; found 342.1349. $C_{22}H_{18}N_2O_2$ (342.4): calcd. C 77.17, H 5.30, N 8.18; found C 76.75, H 4.88, N 7.89.

Quinoxaline 6d: ^{1}H NMR (200 MHz, $CDCl_3$): δ = 8.45 (s, 2 H), 8.15 (s, 2 H), 7.93 (d, J = 8.2 Hz, 4 H), 7.78 (d, J = 8.4 Hz, 4 H) ppm. ^{13}C NMR (75 MHz, [D_6]DMSO): δ = 152.6, 147.3, 134.7, 131.1, 119.1, 112.5 ppm. FTIR (KBr): $\tilde{\nu}$ = 2533, 2119, 2053, 1591, 1547, 1494, 1428, 807 cm^{-1}. M.p. 240 °C. HRMS: calcd. for $C_{22}H_{12}N_4$ 332.1062, found 332.1051. $C_{22}H_{12}N_4$ (332.4): calcd. C 79.50, H 3.64, N 16.86; found C 79.05, H 3.27, N 16.52.

Benzothiadiazole 7a: ^{1}H NMR (200 MHz, $CDCl_3$): δ = 8.23 (d, J = 6.4 Hz, 2 H), 7.97–7.24 (m, 10 H) ppm. ^{13}C NMR (50 MHz, $CDCl_3$): δ = 137.3, 136.5, 133.9, 133.2, 113.8, 113.0 ppm. FTIR (KBr): $\tilde{\nu}$ = 1586, 1463, 1424, 1333 cm^{-1}. M.p. 127 °C. $C_{18}H_{12}N_2S$ (288.4): calcd. C 74.97, H 4.19, N 9.71; found C 75.31, H 4.56, N 9.97.

Benzothiadiazole 7b: ^{1}H NMR (200 MHz, $CDCl_3$): δ = 7.91–7.80 (m, 4 H), 7.79–7.44 (m, 2 H), 7.21–7.10 (m, 4 H) ppm. ^{13}C NMR (50 MHz, $CDCl_3$): δ = 164.50, 161.3, 153.9, 133.3, 132.2, 131.0, 130.9, 128.1, 127.9, 115.9, 115.7, 115.6, 115.5, 113.2 ppm. FTIR (KBr): $\tilde{\nu}$ = 3068, 1604, 1517, 1227, 1163 cm^{-1}. M.p. 127 °C. HRMS: calcd. for $C_{18}H_{10}F_2N_2S$ 324.0532; found 324.0572. $C_{18}H_{10}F_2N_2S$ (324.3): calcd. C 66.65, H 3.11, N 8.64; found C 66.95, H 3.31, N 8.92.

Benzothiadiazole 7c: ^{1}H NMR (200 MHz, [D_6]DMSO): δ = 3.89 (s, 6 H), 7.08 (d, J = 8.4 Hz, 4 H), 7.70 (s, 2 H), 7.32 (d, J = 8.2 Hz, 4 H) ppm. ^{13}C NMR (50 MHz, $CDCl_3$): δ = 159.6, 154.1, 132.2, 130.3, 129.9, 127.4, 114.0, 55.4 ppm. FTIR (KBr): $\tilde{\nu}$ = 3029, 2954, 1604, 1519, 1284 cm^{-1}. M.p. 207 °C. $C_{20}H_{16}N_2O_2S$ (348.4): calcd. C 68.94, H 4.63, N 8.04; found C 69.31, H 4.96, N 8.41.

Benzothiadiazole 7d: ^{1}H NMR (200 MHz, $CDCl_3$): δ = 8.10–7.77 (m, 10 H) ppm. ^{13}C NMR (50 MHz, $CDCl_3$): δ = 152.9, 152.5, 141.2, 140.9, 134.5, 132.8, 132.4, 132.3, 129.8, 129.7, 128.9, 128.5, 127.9, 118.7, 118.6, 116.3, 114.9, 113.8 112.2 ppm. FTIR (KBr): $\tilde{\nu}$ = 3080, 2924, 2862, 2367, 2222, 1747, 1607, 1401, 1185, 826 cm^{-1}. M.p. 160 °C. HRMS: calcd. for $C_{20}H_{10}N_4S$ 338.0626; found 338.0661. $C_{20}H_{10}N_4S$ (338.4): calcd. C 70.99, H 2.98, N 16.56; found C 71.28, H 3.32, N 16.84.

Supporting Information (see also the footnote on the first page of this article): UV/Vis, fluorescence, solid state, and HRMS spectra of all compounds are available.

Acknowledgments

This work was sponsored by grants from CNPq and FAPERGS. BADN, FSM, and ASL also thank the CNPq for fellowships. We also thank Prof. John Spencer (UK) for a critical reading of the manuscript.

[1] M. T. Lee, C. K. Yen, W. P. Yang, H. H. Chen, C. H. Liao, C. H. Tsai, C. H. Chen, *Org. Lett.* **2004**, *6*, 1241–1244.
[2] S. A. Odom, S. R. Parkin, J. E. Anthony, *Org. Lett.* **2003**, *5*, 4245–4248.
[3] L. S. Hung, C. H. Chen, *Mater. Sci. Eng. R* **2002**, *39*, 143–222.
[4] W. J. Shen, R. Dodda, C. C. Wu, F. I. Wu, T. H. Liu, H. H. Chen, C. H. Chen, C. F. Shu, *Chem. Mater.* **2004**, *16*, 930–934.
[5] M. Strukelj, F. Papadimitrakopoulos, T. M. Miller, L. J. Rothberg, *Science* **1995**, *267*, 1969–1972.
[6] C. S. Wang, G. Y. Jung, Y. L. Hua, C. Pearson, M. R. Bryce, M. C. Petty, A. S. Batsanov, A. E. Goeta, J. A. K. Howard, *Chem. Mater.* **2001**, *13*, 1167–1173.
[7] A. R. Brown, D. D. C. Bradley, J. H. Burroughes, R. H. Friend, N. C. Greenham, P. L. Burn, A. B. Holmes, A. Kraft, *Appl. Phys. Lett.* **1992**, *61*, 2793–2795.
[8] C. J. Tonzola, M. M. Alam, W. Kaminsky, S. A. Jenekhe, *J. Am. Chem. Soc.* **2003**, *125*, 13548–13558.
[9] A. P. Kulkarni, Y. Zhu, S. A. Jenekhe, *Macromolecules* **2005**, *38*, 1553–1563.

 © 2006 Wiley-VCH Verlag GmbH & Co. KGaA, Weinheim

[10] P. Karastatiris, J. A. Mikroyannidis, I. K. Spiliopoulos, A. P. Kulkarni, S. A. Jenekhe, *Macromolecules* **2004**, *37*, 7867–7878.
[11] K. R. J. Thomas, M. Velusamy, J. T. Lin, C. H. Chuen, Y. T. Tao, *Chem. Mater.* **2005**, *17*, 1860–1866.
[12] T. Yamamoto, K. Sugiyama, T. Kushida, T. Inoue, T. Kanbara, *J. Am. Chem. Soc.* **1996**, *118*, 3930–3937.
[13] Y. Cui, X. Zhang, S. A. Jenekhe, *Macromolecules* **1999**, *32*, 3824–3826.
[14] I. Starke, G. Sarodnick, V. V. Ovcharenko, K. Pihlaja, E. Kleinpeter, *Tetrahedron* **2004**, *60*, 6063–6078.
[15] Z. J. Zhao, D. D. Wisnoski, S. E. Wolkenberg, W. H. Leister, Y. Wang, C. W. Lindsley, *Tetrahedron Lett.* **2004**, *45*, 4873–4876.
[16] C. W. Ong, S. C. Liao, T. H. Chang, H. F. Hsu, *J. Org. Chem.* **2004**, *69*, 3181–3185.
[17] S. V. More, M. N. V. Sastry, C. C. Wang, C. F. Yao, *Tetrahedron Lett.* **2005**, *46*, 6345–6348.
[18] L. S. Mao, H. Sakurai, T. Hirao, *Synthesis* **2004**, 2535–2539.
[19] M. S. Khan, M. K. Al-Suti, M. R. A. Al-Mandhary, B. Ahrens, J. K. Bjernemose, M. F. Mahon, L. Male, P. R. Raithby, R. H. Friend, A. Kohler, J. S. Wilson, *Dalton Trans.* **2003**, 65–73.
[20] D. Aldakov, M. A. Palacios, P. Anzenbacher, *Chem. Mater.* **2005**, *17*, 5238–5241.
[21] H. Sakurai, M. T. S. Ritonga, H. Shibatani, T. Hirao, *J. Org. Chem.* **2005**, *70*, 2754–2762.
[22] T. Suzuki, M. Saito, H. Kawai, K. Fujiwara, T. Tsuji, *Tetrahedron Lett.* **2004**, *45*, 329–333.
[23] O. Hinsberg, *Ber. Dtsch. Chem. Ges.* **1889**, *22*, 2895–2902.
[24] L. M. Weinstock, P. Davis, B. Handelsman, R. J. Tull, *J. Org. Chem.* **1967**, *32*, 2823–2829.
[25] A. P. Komin, R. W. Street, M. Carmack, *J. Org. Chem.* **1975**, *40*, 2749–2752.
[26] K. Pilgram, M. Zupan, R. Skiles, *J. Heterocycl. Chem.* **1970**, *7*, 629–633.
[27] D. Russowsky, B. A. D. Neto, *Tetrahedron Lett.* **2004**, *45*, 1437–1440.
[28] D. Russowsky, B. A. D. Neto, *Tetrahedron Lett.* **2003**, *44*, 2923–2926.
[29] R. Naef, H. Balli, *Helv. Chim. Acta* **1978**, *61*, 2958–2973.
[30] E. J. Corey, F. N. M. Kuhnle, *Tetrahedron Lett.* **1997**, *38*, 8631–8634.
[31] B. A. D. Neto, A. S. Lopes, M. Wust, V. E. U. Costa, G. Ebeling, J. Dupont, *Tetrahedron Lett.* **2005**, *46*, 6843–6846.
[32] Q. Fang, A. Tanimoto, T. Yamamoto, *Synth. Met.* **2005**, *150*, 73–78.
[33] G. R. Rosa, G. Ebeling, J. Dupont, A. L. Monteiro, *Synthesis* **2003**, 2894–2897.
[34] J. Dupont, C. S. Consorti, J. Spencer, *Chem. Rev.* **2005**, *105*, 2527–2571.
[35] B. A. D. Neto, A. S. A. Lopes, G. Ebeling, R. S. Goncalves, V. E. U. Costa, F. H. Quina, J. Dupont, *Tetrahedron* **2005**, *61*, 10975–10982.
[36] K. Masui, A. Mori, K. Okano, K. Takamura, M. Kinoshita, T. Ikeda, *Org. Lett.* **2004**, *6*, 2011–2014.
[37] C. A. Briehn, M. S. Schiedel, E. M. Bonsen, W. Schuhmann, P. Bauerle, *Angew. Chem. Int. Ed.* **2001**, *40*, 4680–4683.
[38] F. Wilkinson, D. J. McGarvey, A. F. Olea, *J. Phys. Chem.* **1994**, *98*, 3762–3769.
[39] R. P. Ortiz, M. C. R. Delgado, J. Casado, V. Hernandez, O. K. Kim, H. Y. Woo, J. T. L. Navarrete, *J. Am. Chem. Soc.* **2004**, *126*, 13363–13376.
[40] K. Susumu, T. V. Duncan, M. J. Therien, *J. Am. Chem. Soc.* **2005**, *127*, 5186–5195.
[41] R. Q. Yang, R. Y. Tian, J. G. Yan, Y. Zhang, J. Yang, Q. Hou, W. Yang, C. Zhang, Y. Cao, *Macromolecules* **2005**, *38*, 244–253.
[42] M. Velusamy, K. R. J. Thomas, J. T. Lin, Y. C. Hsu, K. C. Ho, *Org. Lett.* **2005**, *7*, 1899–1902.
[43] T. Kanbara, T. Yamamoto, *Macromolecules* **1993**, *26*, 3464–3466.

Received: April 28, 2006
Published Online: September 7, 2006

 © 2006 Wiley-VCH Verlag GmbH & Co. KGaA, Weinheim